54

THE EFFECTS OF GAUSSIAN NOISE ON THE FREQUENCY RESPONSE CHARACTERISTICS OF A NONLINEAR FEEDBACK CONTROL SYSTEM

ASIM K. SEN

Institute of Radio Physics and Electronics, University of Calcutta

(*Received September* 15, 1964)

ABSTRACT. In this paper, a quasi-linearisation technique is described which gives a parameter for approximately representing a memory-type nonlinearity on the basis of an input containing a sinusoidal signal and a Gaussian noise with mean value zero. The parameter is termed 'complex equivalent gain' and this is used for investigating the effects of a Gaussian noise on the frequency response characteristics of a stable feedback control system incorporating the nonlinearity. A simple second-order position control system with backlash in the output coupling is considered as an example and the results obtained are verified experimentally with the help of an electronic analogue computer.

INTRODUCTION

When the input of a stable feedback control system incorporating a memory-type nonlinearity is subjected to a sinusoidal signal, the frequency response characteristics of the system can be determined approximately by the use of linearisation techniques (Stein and Thaler 1958, Sen, 1964). In the application of these techniques, a quasi-linearised transfer function is used to represent the nonlinear element in the system which is called 'complex describing function'.

But, when the input of the nonlinear system considered becomes contaminated with a Gaussian noise then it is found that all the parameters of the frequency response characteristics, namely, the bandwidth, resonant frequency and the height of the resonant peak previously obtained for a particular value of the impressed sinusoidal amplitude, change considerably. This is due to the fact that the transmission property of the nonlinearity alters due to the presence of the noise. In this paper, an analytical method will be proposed for investigating these effects of the Gaussian noise on the frequency response characteristics of a memory-type nonlinear system, where the nonlinearity considered is assumed to be amplitude-sensitive alone. The importance of this investigation arises from the fact that the inputs of all practical control systems are usually contaminated with such external disturbances.

In order to carry out the above analytical investigation, a quasi-linearisation technique will be adopted in which a 'complex equivalent gain' (Sen, 1955) will be obtained for making an approximate representation of the nonlinearity under

the assumption that the input is composed of only a sinusoidal signal and a Gaussian noise with mean value zero. An outline of the proposed quasi-linearisation technique has been presented in the following section.

THE PROPOSED QUASI-LINEARISATION TECHNIQUE

When a linear element is subjected to an input consisting of a sine wave and a Gaussian signal of mean value zero it is found that the response of the element will also contain only the components of the input signal and the original shape of the input wave will be maintained at the output. But, when the element becomes nonlinear, distortion will appear in the shape of the output wave and it will become difficult to make any rigorous analysis of the response of the element in this case. However, it can be seen that, for the assumed input, the response of the nonlinearity can be separated into two parts—one representing the correlated component that exactly reproduces the input spectrum, while the remainder is called the 'distortions' comprising the harmonics and intermodulation components and then a quasi-linearisation technique can be adopted to make an approximate representation of the nonlinearity. The use of this linearisation technique assumes the presence of only the correlated component at the output and defines a quasi-linearised transfer function for the nonlinearity that relates the input to the output correlated component. For the case of nonlinearities that involve memory, phase-shift will be introduced to each of the frequency components at the output and therefore, in such cases, the quasi-linearised transfer function obtained for the nonlinearity becomes a complex quantity and may be called 'complex equivalent gain'. The magnitude of this complex equivalent gain is given by the ratio of the r.m.s. value of the output correlated component to that of the input, while the phase is assumed to be frequency-independent. The above definition of a 'complex equivalent gain' has been made for a memory type nonlinearity under the assumption that the components of the signal assumed at the input of the nonlinearity lie within a narrowband frequency spectrum.

In order to determine the phase function attributed to the quasi-linearised model of the nonlinearity, the simple procedure as outlined below is to be adopted. Consider a nonlinear element (Fig. 1), the input of which is impressed upon by a signal z comprising a sine wave $z_1 = A_z \sin \omega_c t$ and a Gaussian noise z_2 having mean value zero and variance σ_n^2. If the component of the Gaussian noise is expressed in the form $z_2 = \sum_{n=0}^{\infty} a_n \sin(\omega_n t + \phi_n)$ where a_n describes the power spectrum of the noise and ϕ_n is randomly distributed with a uniform probability distribution from 0 to 2π, then, neglecting the harmonics and intermodulation components, the approximate output of the nonlinearity can be written as :

$$y = |H(\sigma)| [A_z \sin \{\omega_c t + \theta(\sigma)\} + \sum_{n=0}^{\infty} a_n \sin \{\omega_n t + \phi_n + \theta(\sigma)\}] \quad \ldots \quad (1)$$

where $|H(\sigma)|$ is the magnitude and $\theta(\sigma)$ the phase of the complex equivalent gain defined for the nonlinearity. In order to attribute the proper sign to the phase function $\theta(\sigma)$, it should be remembered that $\theta(\sigma)$ is negative for those nonlinearities that introduce a lagging phase-shift to the output frequency components for a sinusoidal input, while it is positive for those introducing a leading phase-shift.

Now, the difference between the approximate output and the input multiplied by the magnitude of the complex equivalent gain is given by

$$\begin{aligned} e &= y - |H(\sigma)|z \\ &= 2|H(\sigma)| \sin \frac{\theta(\sigma)}{2} \left[A_z \cos \left\{ \omega_e t + \frac{\theta(\sigma)}{2} \right\} \right. \\ &\qquad \left. + \sum_{n=0}^{\infty} a_n \cos \left\{ \omega_n t + \phi_n + \frac{\theta(\sigma)}{2} \right\} \right] \qquad \ldots (2) \end{aligned}$$

or, the rms value of the quantity e is given by

$$\sigma_e = 2|H(\sigma)|\sigma_z \sin \frac{\theta(\sigma)}{2} \qquad \ldots (3)$$

whence

$$\theta(\sigma) = 2 \sin^{-1} \frac{\sigma_e}{2|H(\sigma)|\sigma_z} \qquad \ldots (4)$$

where σ_z represents the rms value of the total signal at the nonlinearity input.

In practice, however, as the magnitude of the complex equivalent gain defined for the nonlinearity, cannot be easily determined, an approximate measure of the parameter can be obtained by taking the ratio of the rms value of the actual output to that of the input of the nonlinearity. Evidently, this measurement will give a somewhat increased value of the parameter $|H(\sigma)|$ due to the presence of the distortion components at the output of the nonlinearity.

Thus, the procedure for having an approximate measure of the complex equivalent gain of a memory-type nonlinearity for the assumed input can be summarised as follows :

(1) The rms values of the input and the output of the nonlinearity are first measured and then the parameter $|H(\sigma)|$ is computed for different rms values of the input.

(2) The rms values of the quantity e are measured for different values of the input by arranging the set-up as shown in Fig. 1, each time using proper value of the quantity $|H(\sigma)|$ obtained from the procedure in step (1).

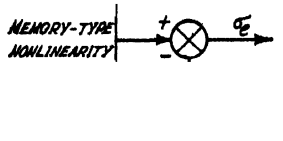

Fig. 1. Set-up for measuring the phase of complex equivalent gain.

(3) Finally, eqn. (4) is used to compute the parameter $\theta(\sigma)$ of the complex equivalent gain.

For different values of the quantities A_z/δ and σ_n/δ the complex equivalent gain of a simple backlash as measured by the above method is presented in Fig. 2, where δ represents the backlash half-width.

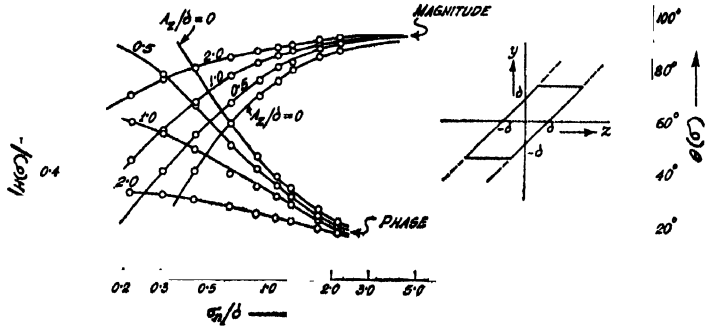

Fig. 2. The complex equivalent gain of a simple backlash.

APPLICATION OF THE PROPOSED QUASI-LINEARISATION TECHNIQUE

In the preceding section, a quasi-linearisation technique has been developed which yields a 'complex equivalent gain' as a parameter for approximately representing a memory-type nonlinearity with an input function comprising a sinusoidal signal and a Gaussian noise with mean value zero. When the nonlinear element considered occurs as a part of a feedback system which is also subjected to a similar input, the application of the quasi-linearisation technique is facilitated by replacing the nonlinearity with the help of the quasi-linearised gain and then the analysis is carried out by obtaining two separate linearised versions for the over-all nonlinear system—one for the sinusoidal portion and the other for the Gaussian component of the impressed signal (Sawaragi and Sugai, 1959). The justification in using the two separate linearised systems for the analysis can be seen from the fact that, in either case, the effect of the remaining signal simultaneously present in the system is included in the quasi-linearised gain obtained for the nonlinearity. Though the presence of the nonlinearity will destroy the nature of the signals impressed upon the system, but it will be assumed that the signal fedback to the input of the nonlinearity will contain only a sinusoidal and a Gaussian component, and, possibly, this assumption will be justified in practice because of the narrow-band characteristic of the feedback system.

A POSITION CONTROL SYSTEM WITH BACKLASH

Consider a position control system as shown in Fig. 3, incorporating backlash in the output coupling and is subjected to a sinusoidal and a Gaussian signal at

the point in the loop as indicated in the figure. Assuming the signal at the input of the nonlinearity to contain only the components of the impressed wave, the

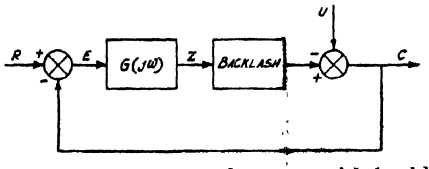

Fig. 3. A position control system with backlash.

application of the quasi-linearisation technique yields the two linearised versions of the nonlinear system as presented in Figs. 4(a) and 4(b).

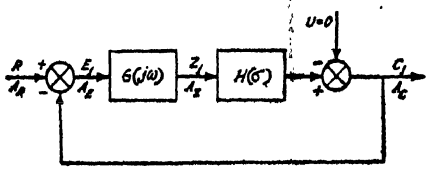

Fig. 4(a). The linearised version of the position control system for sinusoidal portion of the impressed input.

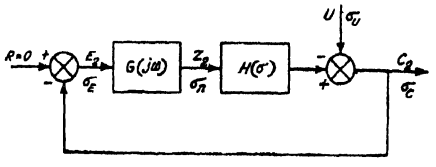

Fig. 4(b). The linearised version of the position control system for Gaussian component of the impressed input.

Confining our attention to the evaluation of the frequency response characteristics of the nonlinear system at the point 'Z' alone, we get from Fig. 4(a),

$$z_1 = \frac{RG(jw)}{1 + H(\sigma)G(jw)} \qquad \ldots (5)$$

while Fig. 4(b) gives

$$\psi z_2(s) = \psi_U(s) \cdot \frac{G(s)}{1 + H(\sigma)\, G(s)} \qquad \ldots (6)$$

where $\psi z_2(s)$ represents the complex frequency spectrum of the Gaussian noise assumed at the point z, which is the input of the nonlinearity and $\psi_U(s)$ is the complex frequency spectrum of the impressed noise. Of the above two equations, it can be readily seen that the first equation gives the required frequency response characteristics of the nonlinear system for different assumed values of the amplitudes of the sine wave and also the Gaussian noise at the input of the nonlinearity, while, with the help of the second equation, the rms values of the impressed noise are computed in terms of the rms noise present at the input point 'Z' of the nonlinearity.

THE USE OF NICHOLS' CHART

When the transfer functions for the linear and the nonlinear part of the system considered are given as plots on the conventional magnitude-phase plane (shown in Fig. 5), then the frequency response characteristics of the closed-loop system

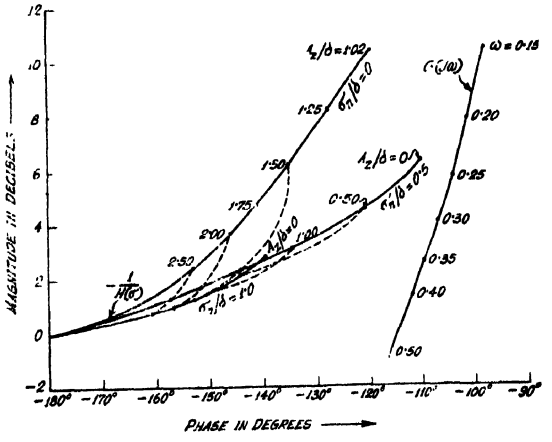

Fig. 5. The magnitude-phase plane plots of the transfer functions for the linear and the nonlinear parts of the position control system.

as given by eqn. (5) can be easily determined by the use of Nichols' chart. Two different approaches can be followed in using the chart as outlined below :

(a) In one approach, the given loci on the magnitude-phase plane are first utilised to obtain different families of curves for the combined transference $H(\sigma)$ $G(j\omega)$ of the linear and the nonlinear components of the system, each family corresponding to a particular value of the rms noise at the input of the nonlinearity. The procedure for obtaining these families of curves for the combined transfer function can be explained as follows :

If the magnitude of the quantity $H(\sigma)\,G(j\omega)$ be expressed in decibels and its phase in degrees, then denoting the respective quantities as $M_{H\omega}$ and $\theta_{H\omega}$, we have

$$M_{H\omega} = |H(\sigma)| + |G(jw)|$$

$$= -\frac{1}{|H(\sigma)|} + |G(jw)| \qquad (7)$$

and

$$Q_{H\omega} = /H(\sigma) + /G(jw)|$$

$$= -\left[\, 180° + \left/ -\frac{1}{H(\sigma)} \right.\right] + /G(jw) \qquad \ldots\ (8)$$

Since the values of the quantities $\frac{1}{|H(\sigma)|}$ and $\left/ \frac{1}{-H(\sigma)} \right.$ are directly obtainable from the loci of $\left/ -\frac{1}{H(\sigma)} \right.$ on the magnitude-phase plane and

are known for the values of the parameters A_z/δ and σ_n/δ marked on these loci, substitution of these values in the above equations gives the values of both the magnitude and phase of the combined transference for different values of the frequency, and thus, the required families of curves are obtained at different selected values of A_z/δ and σ_n/δ, each curve being graduated with different values of the frequency.

For a particular selected value of the rms noise σ_n/δ and with different values of A_z/δ as a parameter, the family of curves obtained for the combined transference are now superimposed on the contour system of a Nichols' Chart and the points of intersection of these curves with the contours on the Nichols' chart are noted which give the frequency response characteristics for the transfer function

$$\frac{A}{B} = \frac{H(\sigma)\ G(jw)}{1+H(\sigma)\ G(jw)} \qquad \ldots \quad (9)$$

at the selected value of σ_n/δ and for the different chosen values of A_z/δ.

The same procedure as outlined above is then followed for different selected values of σ_n/δ.

Knowing the frequency response characteristics for the transfer function A/B with the help of the Nichols' chart, the frequency response characteristics of the system given by eqn. (5) can now be easily computed and this can be done by determining the values of the parameter $H(\sigma)$ from Fig. 5 at the different selected values of σ_n/δ and A_z/δ and by substituting those values in the relation :

$$\frac{Z_1}{R} = \frac{A}{B} \cdot \frac{1}{H(\sigma)} \qquad \ldots \quad (10)$$

(b) In the other approach, on the other hand, as suggested by Stein and Thaler (1958), the contour system of the Nichol's chart is superimposed on the given plots of the transfer function of the system, locating its origin on the selected values of σ_n/δ and A_z/δ as marked on the $\left[-\frac{1}{H(\sigma)}\right]$-loci and the same results as represented in eqn. (9) are obtained by observing the points of intersection between the chart-contour and the locus of the given linear transference $G(jw)$ of the system considered. It should be noted, however, that though this latter approach will be useful only when the Nichols' chart is available as contours drawn on a transparent template, but it will be more convenient because of the fact that the laborious computation of the families of curves for the combined transference $H(\sigma)\ G(jw)$ will not be required in this case.

AN EXAMPLE OF A SECOND-ORDER SYSTEM WITH BACKLASH

If the position control system considered in the preceding section be of second order with its linear part having the transfer function $G(jw) = K_v/jw(jw+1)$, then the family of curves for the combined transfer function $H(\sigma)\ G(jw)$ obtained

at a selected value of σ_n/δ and superimposed on the Nichols' chart will be as shown in Fig. 6. Taking the value of the velocity error constant $K_v = 0.5$, the amplitude

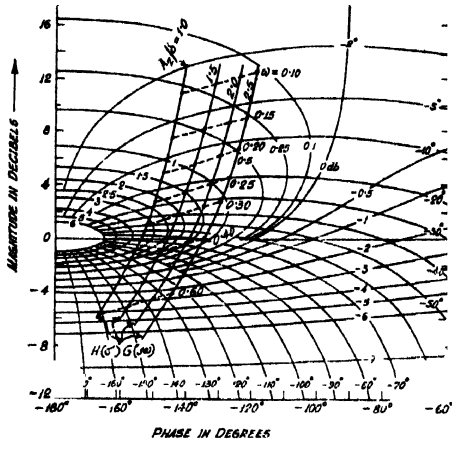

Fig. 6. The loci of the combined transfer function for the linear and nonlinear components of a second-order system superimposed on the contour system of a Nichols' chart.

and the phase response characteristics of the system have been evaluated for different chosen values of σ_n/δ and A_z/δ and the particular characteristics obtained for $\sigma_n/\delta = 0.5$ and for a set of selected values of A_z/δ are presented in Figs. 7 and 8, respectively, where A_z/A_R represents the amplitude response and ϕ_z the phase response of the system at the point Z. With the help of these characteristics evaluated at different constant values of A_z/δ, the frequency response characteristics of the system can be easily determined for different constant values of the amplitude A_R/δ of the sinusoidal signal impressed upon the system and this can be done by first designating at each position of the amplitude response characteristics obtained above with the proper value of A_R/δ and then drawing the locus

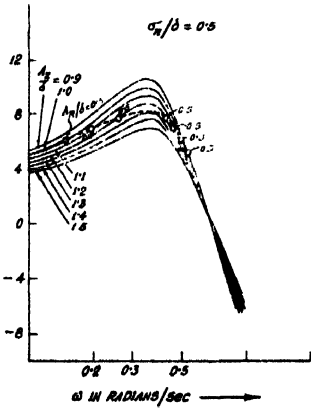

Fig. 7. The amplitude response characteristics of the second-order system for $\sigma_n/\delta = 0.5$ and for $A_z/\delta = 0.9, 1.0, 1.1, 1.2, 1.3, 1.4, 1.5$. (The dotted curve shows the corresponding amplitude response characteristics for $A_R/\delta = 0.5$).

of constant-A_R/δ on these characteristics. This is illustrated in Fig. 7. Knowing from the figure the values of w and A_z/δ at different positions on the constant

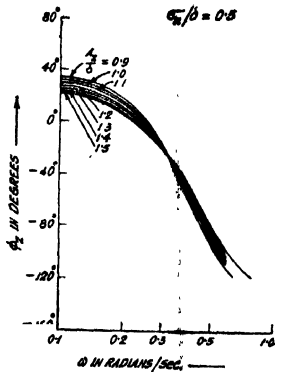

Fig. 8. The phase response characteristics of the second-order system for $\sigma_n/\delta = 0.5$ and for $A_z/\delta = 0.9$, 1.0, 1.1, 1.2, 1.3, 1.4, 1.5.

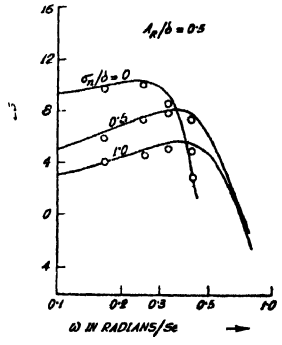

Fig. 9. The amplitude response characteristics of the second-order system for $A_R/\delta = 0.5$ and for $\sigma_n/\delta = 0$, 0.5 and 1.0.
– analytical values
⊙experimental values.

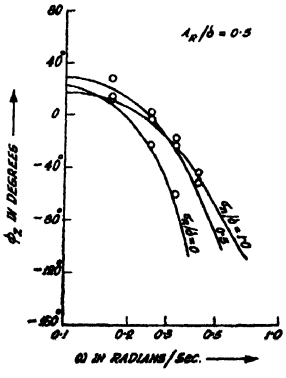

Fig. 10. The phase response characteristics of the second-order system for $A_R/\delta = 0.5$ and for $\sigma_n/\delta = 0$, 0.5 and 1.0.
– analytical values.
⊙experimental values.

A_R/δ locus, the corresponding phase response characteristics of the system is then determined with the help of Fig. 8. Thus the amplitude and the phase response characteristics of the system are determined for different constant values of A_R/δ and the characteristics evaluated at $A_R/\delta = 0.5$ and for a set of selected values of σ_n/δ are presented in Figs. 9 and 10, respectively.

Since, in the present system considered, the noise impressed upon the system occurs at the output point C, the rms values of the impressed noise corresponding to the different selected values of the rms noise at the point Z are to be determined and this will be done by the use of eqn. (6). Substituting the expression for $G(jw)$, eqn. (6) can be written as

$$\psi_{Z_2}(s) = \psi_U(s) \cdot \frac{K_v}{s(s+1)+K_v H(\sigma)} \qquad \ldots (11)$$

Therefore, for a particular input spectrum given by

$$\psi_U(w) = \frac{\omega_0 n}{j\omega+\omega_0} \cdot \frac{\omega_0 n}{-j\omega+\omega_0} \qquad \ldots (12)$$

where $s = jw$ and ω_0 is the half-power frequency and n the low frequency amplitude of the noise spectrum, the normalised values of the impressed rms noise in terms of the rms noise at the point z are obtained from the relation :

$$\frac{\sigma_U}{\delta} = \frac{\sigma_n}{\delta} \sqrt{\left| \frac{H(\sigma)}{K_v} \left\{ \omega_0 + \frac{K_v}{\omega_0+1} H(\sigma) \right\} \right|} \qquad \ldots (13)$$

Since the parameter $H(\sigma)$ in the above equation is determined by the values of both σ_n/δ and A_z/δ, a set of curves are drawn for the particular system considered by plotting the different values of σ_n/δ as abscissa and the corresponding values of σ_u/δ as ordinate and taking the values of A_z/δ as a parameter. This is shown in Fig. 11. With the help of these curves, it will be possible to obtain the values of σ_U/δ corresponding to the selected values of σ_n/δ and A_z/δ in the above

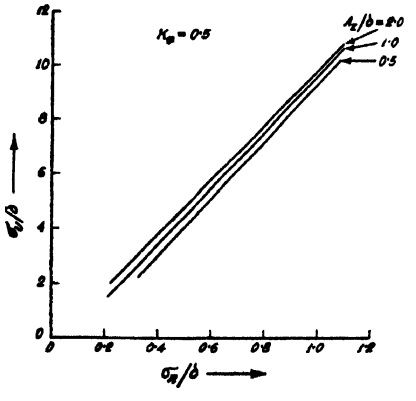

Fig. 11. The plots of σ_U/δ vs. σ_n/δ with different values A_z/δ as a parameter.

analysis or, conversely, for a given value of σ_u/δ, the values of σ_n/δ and $A_z/\delta c$ an also be selected with the help of these curves.

COMPUTER STUDY

In order to have an experimental check on the results obtained analytically, the nonlinear system considered in the example, is simulated on an electronic analogue computer and the arrangements as shown in Fig. 12, is made for measur-

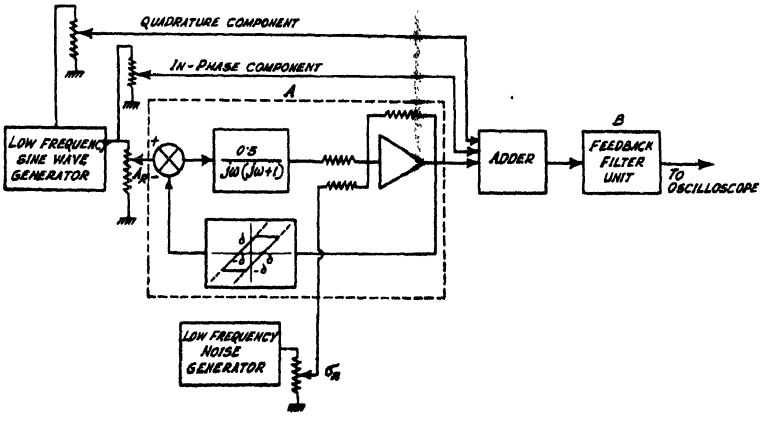

Fig. 12. The experimental arrangement for measuring the amplitude and phase response characteristics of the second-order system with noise injected at the nonlinearity input.

ing both the amplitude and the phase response characteristics of the system for different values of the rms noise present at the point Z in the system loop.

In the arrangement, the block A is the simulated system, under investigation, where the output terminal represents the point Z in the system loop at which the frequency response characteristics are proposed to be evaluated. The block B represents a feedback filter unit having a very narrow pass-band around a centre frequency equal to ω_c and the centre frequency is ganged to the frequency of the oscillator supplying the sinusoidal signal impressed upon the input of the simulated system. The filter unit will be used in conjunction with an oscilloscope for detection of the condition of balance of the fundamental component of the impressed sine wave present at the output of the simulated system.

The procedure adopted for the measurement can be outlined as follows : First of all, the amplitude of the sine wave of a particular frequency and also the rms value of noise impressed upon the system is set at the selected values and then the fundamental component appearing at the output of the simulated system due to the impressed sine wave is balanced out by the addition of suitable fractions of the in-phase and quadrature -components of the same sinusoidal signal and the balance is detected with the help of the oscilloscope. As the output

point of the simulated system will be contaminated with noise, the point of exact balance will not correspond to zero output of the filter unit, but, instead, a low frequency noise component will appear on the oscilloscope due to the finite bandwidth of the filter. However, the adjustments could be made such that the departure from the point of balance could readily be detected for a few millivolts change in the fundamental balancing signal from the value at which the balance is obtained. Finally, the amplitude values of the in-phase and the quadrature components of the fundamental balancing signal corresponding to the point of balance are noted and these are used for computing the required amplitude and phase response of the system at the particular value of the frequency of the impressed sine wave.

The above procedures are then repeated for different frequencies and at different selected rms values of the impressed noise and the results obtained are presented and are indicated as circles on Figs. 9 and 10.

CONCLUSION

The quasi-linearisation technique described in the first part of this paper has been found to be useful for investigating the effect of a Gaussian noise on the frequency response characteristics of a feedback control system incorporating a memory-type nonlinearity. As a graphical aid to the evaluation of the closed-loop equation for obtaining the frequency response characteristics of the system, Nichols' chart has been used and the two possible ways of using the chart have been outlined. It has been observed that, by assuming the Gaussian noise to be impressed at the input of the nonlinearity, the effect of the rms noise is to decrease both the amplitude and the phase response characteristics of the system at the lower frequencies, while increasing them towards the high frequency end of the characteristics. The experimental results obtained from a computer study of the system are found to corroborate the above observations.

ACKNOWLEDGMENT

The author is grateful to Prof. J. N. Bhar, D.Sc., F.N.I., for his keen interest in the work and to Dr. A. K. Choudhury, M.Sc., D.Phil. for his guidance and many helpful suggestions and discussions. The author also thankfully acknowledges the award of a research fellowship by the Council of Scientific and Industrial Research, New Delhi.

REFERENCES

Stein, W. A. and Thaler, G. J., 1958, *Trans. A.I.E.E.*, **77**, Part 2, 91–96.

Sen, A. K., 1964, *Control*, **8**, 77, 566-569.

Sen, A. K., 1965, *Trans. I.E.E.E. on Automatic Co trol*, to be published.

Sawaragi, Y. and Sugai, N., 1959, *Memoirs of the Faculty of Engineering*, Kyoto University, Vol. XXI, Part 2,

DETERMINATION OF THE DIELECTRIC CONSTANT OF A TUBULAR MATERIAL AT 3KMc/s

S. K. SEN, J. BASU* AND A. K. GHOSHAL

INSTITUTE OF RADIO PHYSICS & ELECTRONICS, UNIVERSITY OF CALCUTTA

(*Received September* 22, 1964)

ABSTRACT. The paper describes two methods for determining the resonant behaviour of cylindrical cavity with a tubular dielectric material introduced coaxially in it The first method tends to give the exact value of the dielectric constant of the material The second one, based on a perturbation theory, yields somewhat approximate results

Experiments carried out at a microwave frequency of 3 KMc/s on two tubes of Pyrex glass, show that the inaccuracy in determining the dielectric constant arising out of the approximation inherent in the perturbation theory, is, in these cases, so small as to be compatible with the inaccuracy due to experimental limitations

INTRODUCTION

The treatment on the resonant behaviour of a cylindrical cavity when partially filled with a solid dielectric rod, has been given by Horner *et al* (1946). With the help of this, an exact evaluation of the dielectric constant of the rod specimen can be made by solving the transcendental equation relating the dielectric constant and the resonant frequency of the cavity with the rod placed coaxially inside. An approximate analysis on the basis of a perturbation theory was also presented by Slater (1946), with which the dielectric constant can be measured from the change in resonant frequency of the cavity with and without the specimen. This analysis can be utilised to measure the dielectric constant of a fluid (liquid, gas or plasma) in a tubular container (Biondi and Brown, 1949); the evaluation of the dielectric constant of the contaner is not required. For an exact evaluation, however, it is necessary to determine the dielectric constant of the container.

In the present work the treatment developed by Horner *et al* (1946), as well as the approximate analysis given by Slater (1946), valid for a solid cylindrical dielectric, are extended for a lossless dielectric in the form of a tube. These methods have been used at a microwave frequency of 3 KMc/s to measure the dielectric constant of two pyrex glass tubes, subsequently to be used as plasma containers.

THEORETICAL CONSIDERATIONS

The cavity is operated in the lowest frequency mode i.e. TM_{010} mode. The boundaries of the cavity are assumed to be perfectly conducting.

* Present Address : Saha Institute of Nuclear Physics, Calcutta

(a) Exact solution

Maxwell's equations valid for the interior of the cavity are, in cylindrical coordinates (z, r, θ). :

$$\left.\begin{aligned} j\omega\mu H_\theta &= \frac{\partial E_z}{\partial r} \\ (\sigma+j\omega k)E_z &= \frac{1}{r}\frac{\partial}{\partial r}(rH_\theta) \end{aligned}\right\} \quad \ldots (1)$$

where μ, k and σ are the permeability, permittivity and conductivity of the homogeneous dielectric medium filling the cavity and ω is the angular frequency. All the parameters are expressed in rationalised *M*.K.S. units.

Solutions of the above equations for E_z and H_θ are :

$$\left.\begin{aligned} E_z &= \frac{K}{\sigma+j\omega k} AJ_0(Kr)e^{j\omega t} \text{ volts/metre} \\ H_\theta &= AJ_1(Kr)e^{j\omega t} \text{ amp/metre} \end{aligned}\right\} \quad \ldots (2)$$

in which J_0, J_1 are the Bessel functions of the first kind, A is the constant of integration governed by the strength of excitation and the propagation constant K is given by

$$K^2 = -j\omega\mu(\sigma+j\omega k) \quad \ldots (3)$$

Let the cavity contain three lossless media ($\sigma = 0$) 1, 2, and 3, having permittivities k_1, k_2, k_3 respectively, as shown in Fig. 1. and permeabilities equal to

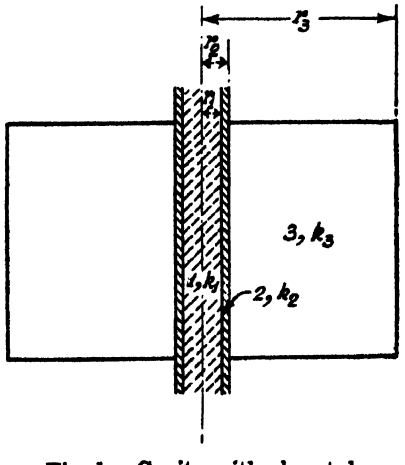

Fig 1 Cavity with glass tube

that of free space, μ_0. The propagation constants for the media are, from eqn. (3),

$$\left.\begin{aligned} K_1 &= \omega\sqrt{\mu_1 k_1} = \omega\sqrt{\mu_0 k_1} = \beta_1(\text{say}) \\ K_2 &= \omega\sqrt{\mu_2 k_2} = \omega\sqrt{\mu_0 k_2} = \beta_2 \\ K_3 &= \omega\sqrt{\mu_3 k_3} = \omega\sqrt{\mu_0 k_3} = \beta_3 \end{aligned}\right\} \quad \ldots (4)$$

Solutions of Maxwell's equations for the electric and magnetic fields, can be written as follows :

For medium *I*

$$\left.\begin{aligned} E_{Z_1} &= \frac{\beta_1}{j\omega k_1} B_1 J_0(\beta_1 r) e^{j\omega t} \\ H_{\theta_1} &= B_1 J_1(\beta_1 r) e^{j\omega t} \end{aligned}\right\} \quad \ldots (5)$$

For medium 2

$$\left.\begin{aligned} E_{Z_2} &= \frac{\beta_2}{j\omega k_2} [B_2 J_0(\beta_2 r) + C_2 Y_0(\beta_2 r)] e^{j\omega t} \\ H_{\theta_2} &= [B_2 J_1(\beta_2 r) + C_2 Y_1(\beta_2 r)] e^{j\omega t} \end{aligned}\right\} \quad \ldots (6)$$

For medium 3

$$\left.\begin{aligned} E_{Z_3} &= \frac{\beta_3}{j\omega k_3} [B_3 J_0(\beta_3 r) + C_3 Y_0(\beta_3 r)] e^{j\omega t} \\ H_{\theta_3} &= [B_3 J_1(\beta_3 r) + C_3 Y_1(\beta_3 r)] e^{j\omega t} \end{aligned}\right\} \quad \ldots (7)$$

Here B's and C's are constants of integration depending upon the strength of excitation and Y_0, Y_1 are the Bessel functions of the second kind. Equation (5) does not contain the second kind Bessel functions as they become infinite at the axis of the cavity.

The boundary conditions for the cavity system are :

(1) The tangential component of the electric field at the cavity wall vanishes.

(2) There is continuity of electric and magnetic fields at the boundaries of the media 3, 2 and 2, 1. Applying these conditions we get from equations (5), (6) and (7)

$$B_3J_0(\beta_3r_3)+C_3Y_0(\beta_3r_3) = 0$$

$$\frac{\beta_3}{k_3}\,[B_3J_0(\beta_3r_2)+C_3Y_0(\beta_3r_2)] = \frac{\beta_2}{k_2}\,[B_2J_0(\beta_2r_2)+C_2Y_0(\beta_2r_2)]$$

$$B_3J_1(\beta_3r_2)+C_3Y_1(\beta_3r_2) = B_2J_1(\beta_2r_2)+C_2Y_1(\beta_2r_2) \qquad (8)$$

$$\frac{\beta_2}{k_2}\,[B_2J_0(\beta_2r_1)+C_2Y_0(\beta_2r_1)] = \frac{\beta_1}{k_1}\,B_1J_0(\beta_1r_1)$$

$$B_2J_1(\beta_2r_1)+C_2Y_1(\beta_2r_1) = B_1J_1(\beta_1r_1)$$

Now, from equation (4)

$$\beta_1 = \beta_3\sqrt{\frac{k_1}{k_3}} \qquad (9)$$

and $$\beta_2 = \beta_3\sqrt{}$$

Eliminating the constants in equation (8) and using eqn. (9), we get the following transcendental equation relating the dielectric constants of the different media.

$$\left[\, J_0(\beta_2r_2)-\sqrt{\frac{k_2}{k_3}}\,FJ_1(\beta_2r_2)\,\right]\left[\, Y_0(\beta_2r_1)J_1(\beta_1r_1)-\sqrt{\frac{k_2}{k_1}}\,J_0(\beta_1r_1)Y_1(\beta_2r_1)\right]$$

$$=\left[\,\sqrt{\frac{k_2}{k_3}}\,FY_1(\beta_2r_2)-Y_0(\beta_2r_2)\,\right]\left[\,\sqrt{\frac{k_2}{k_1}}\,J_0(\beta_1r_1)J_1(\beta_2r_1)-J_0(\beta_2r_1)J_1(\beta_1r_1)\right] \ldots (10)$$

where $$F = \frac{J_0(\beta_3r_2)Y_0(\beta_3r_3)-J_0(\beta_3r_3)Y_0(\beta_3r_2)}{J_1(\beta_3r_2)Y_0(\beta_3r_3)-J_0(\beta_3r_3)Y_1(\beta_3r_2)}$$

Assuming that the medium 3 is air, we get a transcendental equation from (10) which gives the dielectric constant of medium 1 in terms of that of 2 and vice versa, provided ω, the resonant frequency of the composite system is known.

Further, if we assume that the dielectric medium 1, enclosed by the tube represented by the medium 2, is air, we can find $k_2/k_0 = \epsilon_2$, the dielectric constant of the tubular material from the following equation, the permittivity of air being taken equal to that of free space, k_0.

$$\left[\, J_0(\beta_2r_2)-\sqrt{\frac{k_2}{k_0}}\,F'J_1(\beta_2r_2)\,\right]\left[\, Y_0(\beta_2r_1)J_1(\beta_0r_1)-\sqrt{\frac{k_2}{k_0}}\,J_0(\beta_0r_1)\,Y_1(\beta_2r_1)\right]$$

$$=\left[\,\sqrt{\frac{k_2}{k_0}}\,F'Y_1(\beta_2r_2)-Y_0(\beta_2r_2)\right]\left[\,\sqrt{\frac{k_2}{k_0}}\,J_0(\beta_0r_1)J_1(\beta_2r_1)-J_0(\beta_2r_1)J_1(\beta_0r_1)\right] \ldots (11)$$

where $$F' = \frac{J_0(\beta_0 r_2)\,Y_0(\beta_0 r_3) - J_0(\beta_0 r_3)\,Y_0(\beta_0 r_2)}{J_1(\beta_0 r_2)\,Y_0(\beta_0 r_3) - J_0(\beta_0 r_3)\,Y_1(\beta_0 r_2)}$$

and $\beta_0 = w\sqrt{\mu_0 k_0} = \frac{w}{c}$, c being the velocity of light in free space.

(b) *Solution based on a Perturbation Theory*

When the electric or magnetic field within a cavity is perturbed by insertion of a material within it, a change occurs in the distribution of the electromagnetic field. Consequently the resonant frequency of the cavity changes. This change of resonant frequency, Δf, is related to the dielectric constant of the material inserted.

Let a dielectric tube be placed coaxially within the cavity. For TM_{010} mode being used, the electric field only is disturbed. Following Slater (1946), the perturbation equation is

$$\frac{\Delta f}{f_0} = -\frac{\int_{v_s}(\epsilon-1)E^2 dv}{\int_{v_c} E^2 dv} \qquad \ldots (12)$$

where f_0 is the resonant frequency and E is the electric field intensity of the unperturbed cavity, Δf is the change in frequency due to the introduction of the tube. v_s refers to integration over the volume of the tube and v_c that over the volume of the cavity. It should, however, be noted that this equation is valid only if the perturbation is small i.e. the dielectric constant of the material under study is not very high and the radius of the tube is small compared to that of the cavity.

Now, using cylindrical coordinates (z, r, θ), the solution of Maxwell's equation for the electric field in a cylindrical cavity operating in TM_{010} mode is, in absence of any perturbation,

$$E = DJ_0(K_0 r) \qquad \ldots (13)$$

where K_0 is the propagation constant and D is a constant of integration depending upon the strength of excitation.

From equations (12) and (13)

$$\frac{\Delta f}{f_0} = -\frac{1}{2}\frac{\int_z\int_r\int_\theta (\epsilon-1)D^2 J_0^2(K_0 r)dr\cdot rd\theta\cdot dz}{\int_z\int_r\int_\theta D^2 J_0^2(K_0 r)dr\cdot rd\theta\cdot dz}$$

$$= -\frac{1}{2}\frac{(\epsilon-1)D^2 2\pi\cdot L\int_{r_1}^{r_2} rJ_c^2(K_0 r)dr}{D^2\cdot 2\pi\cdot L\int_0^{r_3} rJ_0^2(K_0 r)dr} \qquad \ldots (14)$$

L represents the length of the cavity . r_1, r_2 are the internal and external radii of the tube and r_3 is the radius of the cavity (Fig. 1).

From epuation (14)

$$\frac{\Delta f}{f_0} = -\frac{1}{2}(\epsilon-1)\frac{\int_{r_1}^{r_2} rJ_0^2(K_0r)dr}{\int_0^{r_3} rJ^0{}_2(K_0r)dr}$$

or,
$$\epsilon = 1 - \frac{2\Delta f}{f_0}\cdot\frac{\int_0^{r_3} rJ_0^2(K_0r)dr}{\int_{r_1}^{r_2} rJ_0^2(K_0r)dr}$$

$$= 1 - \frac{2\Delta f}{f_0}\cdot\frac{r_3^2[J_0^2(K_0r_3)+J_1^2(K_0r_3)]}{r_2^2[J_0^2(K_0r_2)+J_1^2(K_0r_2)]-r_1^2[J_0^2(K_0r_1)+J_1^2(k_0r_1)]} \quad \ldots \quad (15)$$

As the cavity wall is assumed to be perfectly conducting, the electric field at $r = r_3$ is zero. Therefore, from eauation (13), $J_0(K_0 r_3) = 0$. Since the cavity is operated in the TM_{010} mode, $K_0 r_3 = 2.405$, the value at which the first zero of J_0 occurs.

Equation (15) becomes

$$\epsilon = 1 - \frac{2\Delta f}{f_0}\cdot\frac{r_3^2[J_1^2(2.405)]}{r_2^2\left[J_0^2\left(2.405\frac{r_2}{r_3}\right)+J_1^2\left(2.405\frac{r_2}{r_3}\right)\right]-r_1^2\left[J_0^2\left(2.405\frac{r_1}{r_3}\right)+J_1^2\left(2.405\frac{r_1}{r_3}\right)\right]} \quad \ldots \quad (16)$$

EXPERIMENT

The block diagram of the experimental arrangement is shown in Fig. 2.

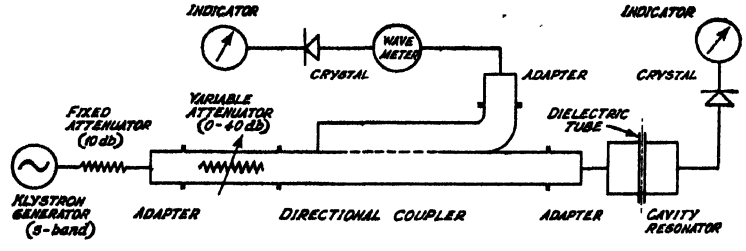

Fig 2 Experimental arrangement.

Two pyrex glass tubes were chosen as dielectric samples and each of them, in turn, was placed coaxially inside the cavity. The resonant frequencies of the cavity with and without each of the samples were measured. The resonant frequency, in each case, is given by the frequency at which the transmission through the cavity is maximum. The frequency meter gives an accurate reading within ± 0.3 Mc/sec.

RESULTS

The resonant frequency of the empty cavity in TM_{010} mode as measured experimentally (f_0') is found to be slightly different from that calculated from its dimensions (f_0). The discrepancy is assumed to be due to the presence of holes in the cavity wall provided for insertion of the samples and the coupling loops. It is therefore evident that the measured resonant frequency of the cavity with a sample (f') is also affected by the holes and needs correction, the corrected value being taken as

$$f = f' + (f_0 - f_0')$$

The frequencies f_0, f_0', f', f and the difference frequency $\Delta f = (f' - f_0')$ are given in Table I.

Radius of the cavity $r_3 = 3.837$ cm.

Sample I. Internal radius, $r_1 = 0.145$ cm
External radius, $r_2 = 0.233$ cm.

Sample II. Internal radius, $r_1 = 0.389$ cm.
External radius, $r_2 = 0.501$ cm.

The internal radii were calculated from the volume of Mercury filling the tubes as described by Worsnop and Flint (1961).

TABLE I

Sample	f_0 Mc/sec	f_0' Mc/sec	f' Mc/sec	f Mc/sec	Δf Mc/sec
I	2992.7	2999.0	2950.7	2944.4	48.3
II	2992.7	3004.5	2874.7	2862.9	129.8

Equation (11) is used for determining the exact value of the dielectric constant of the samples, puttng $\omega = 2\pi f$ where f is obtained from Table I. With the help of equation (16) based on the perturbation theory, the dielectric constant is again calculated; f_0 and Δf are given by Table I. Dielectric constant for two pyrex glass tubes as determined by the above methods, are recorded in Table II. Its percentage deviation for the solution based on the perturbation theory, with respect to the value obtained from the exact solution, is also recorded.

TABLE II

Sample	Dielectric constant		percentage deviation $\frac{b-a}{a} \times 100\%$
	from exact solution a	from perturbation theory b	
I	4.80	4.86	1.25
II	4.58	4.59	0.22

CONCLUDING REMARKS

The value of the dielectric constant of pyrex glass is found to be in conformity with that reported earlier (Von Hippel, 1954; Forsythe, 1956; Knoll, 1959). It appears from Table II that the composition of the two tube samples is slightly different.

The result for the tubes, as obtained from the solution based on the perturbation theory, differs, by less than 2%, from that given by the exact solution. It may be concluded that the inaccuracy due to the approximation inherent in the perturbation method is, in these cases, so small as to be compatible with the inaccuracy due to experimental limitations. However, if the perturbation is large, i.e., if the material under study is of high dielectric constant or if the thickness of the tubewall is appreciable, compared to the radius of the cavity resonator, the perturbation theory fails to hold. The exact method described in section (a) of theoretical consideration would, then, have to be followed.

The dielectric material discussed in this paper is assumed to be completely lossless. For a material with a low loss tangent, the methods described for determining the dielectric constant may still be applicable with a fair degree of accuracy; the loss tangent can be determined by measuring the 'Q' of the cavity with and without the specimen and applying, in an extended form, the perturbation method (Slater, 1946) or, for a more accurate evaluation, the method described by Horner *et al* (1946).

ACKNOWLEDGMENT

The authors are indebted to Prof. J. N. Bhar, D.Sc., F.N.I., for his keen interest in the work and for valuable discussions.

REFERENCES

Biondi, M. A., and Brown, S. C., 1949, *Phys. Rev.* **75**, 1700

Forsythe, William Elmer, 1956, Smithsonian Physicel Tablos, Smithsonian Institution, Washington, 534

Horner, F., Taylor, T. A., Dunsmuir, R., Lamb, T., and Jackson, Willis, 1946, *Jour Inst Elec Eng*, **93**, Part III, 53

Knoll, Max., 1959 Materials and Processes of Electron Devices, Springer-Verlag, Berlin/Göttingen/Heidelberg, 219

Slater, J. C., 1946, *Review of Modern Physics*, **18**, 441

Von Hippel., Arthur R., 1954, Dielectric Materials and Applications, Technology Press of M I T and John Wiley and Sons, Inc., New York, 310

Worsnop, B. L., and Flint, H. T., 1961, Advanced Practical Physics for Students, Methuen and Co. Ltd., London, 26.